

Statistical mechanics of neocortical interactions: Nonlinear columnar electroencephalography

Lester Ingber

Lester Ingber Research
Ashland Oregon USA
ingber@ingber.com, ingber@alumni.caltech.edu
<http://www.ingber.com/>

ABSTRACT: Columnar firings of neocortex, modeled by a statistical mechanics of neocortical interactions (SMNI), are investigated for conditions of oscillatory processing at frequencies consistent with observed electroencephalography (EEG). A strong inference is drawn that physiological states of columnar activity receptive to selective attention support oscillatory processing in observed frequency ranges. Direct calculations of the Euler-Lagrange (EL) equations which are derived from functional variation of the SMNI probability distribution, giving most likely states of the system, are performed for three prototypical Cases, dominate excitatory columnar firings, dominate inhibitory columnar firings, and in-between balanced columnar firings, with and without a Centering mechanism (CM) (based on observed changes in stochastic background of presynaptic interactions) which pulls more stable states into the physical firings ranges. Only states with the CM exhibit robust support for these oscillatory states. These calculations are repeated for the visual neocortex, which has twice as many neurons/minicolumn as other neocortical regions. These calculations argue that robust columnar support for common EEG activity requires the same columnar presynaptic parameter necessary for ideal short-term memory (STM). It is demonstrated at this columnar scale, that both shifts in local columnar presynaptic background as well as local or global regional oscillatory interactions can effect or be affected by attractors that have detailed experimental support to be considered states of STM. Including the CM with other proposed mechanisms for columnar-glia interactions and for glial-presynaptic background interactions, a path for future investigations is outlined to test for quantum interactions, enhanced by magnetic fields from columnar EEG, that directly support cerebral STM and computation by controlling presynaptic noise. This interplay can provide mechanisms for information processing and computation in mammalian neocortex.

KEYWORDS: EEG; short term memory; nonlinear; statistical

Most recent drafts are available as http://www.ingber.com/smni09_nonlin_column_eeg.pdf .

This paper was published in

%A L. Ingber

%T Statistical mechanics of neocortical interactions: Nonlinear columnar electroencephalography

%J NeuroQuantology Journal

%V 7

%N 4

%P 500-529

%D 2009

%O URL <http://www.neuroquantology.com/journal/index.php/nq/article/view/365/385>

\$Id: smni09_nonlin_column_eeg.v 1.134 2009/12/12 22:28:32 ingber Exp ingber \$

1. Origins of EEG

The origins and utility of observed electroencephalography (EEG) are not yet clear, i.e., Delta (> 0-4 Hz), Theta (4-7 Hz), Alpha (8-12 Hz), Beta (12-30 Hz), and Gamma (30-100+ Hz). Some studies strongly dismiss the notion that EEG is an epiphenomenon, and that such oscillations may be causal in information processing in the brain (Alexander, 2007; Alexander, Arns, Paul, Rowe, Cooper, Esser *et al*, 2006; Radman, Su, An, Parra & Bikson, 2007). Several studies strongly link the presence of oscillatory processing during short-term (STM) and long-term memory (LTM) formation, e.g., Gamma facilitating STM formation, and Theta facilitating LTM (Axmacher, Mormann, Fernandez, Elger & Fell, 2006; Jensen & Lisman, 2005; Kahana, 2006; Kahana, Seelig & Madsen, 2001; Lisman & Idiart, 1995; Logar, Belìe, Koritnik *et al*, 2008; Meltzer, Fonzo & Constable, 2009; Mormann, Fell, Axmacher *et al*, 2005; Osipova, Takashima, Oostenveld, Fernandez, Maris & Jensen, 2006; Sederberg, Kahana, Howard *et al*, 2003; Singer, 1999).

Many neuroscientists believe that global regional activity supports such wave-like oscillatory observations (Nunez, 1974; Nunez, 1981; Nunez, 1995). Here, regional refers to major neocortical regions, e.g., visual, auditory, somatic, associative, frontal, etc. Global refers to interactions among these regions.

Some other investigators have shown how reasonable models of relatively local columnar activity can support oscillatory interactions, using linearized dispersion relations derived from SMNI (Ingber, 1983; Ingber, 1985a). Here, local refers to scales of interactions among neurons across columns consisting of hundreds of neurons and macrocolumns consisting of thousands of minicolumns. This local approach, using a statistical mechanics of neocortical interactions (SMNI) has also included global regional interactions among distant local columnar activity (Ingber & Nunez, 1990).

Nature has developed structures at intermediate scales in many biological as well as in many non-biological systems to facilitate flows of information between relatively small and large scales of activity. Many systems possess such structures at so-called mesoscopic scales, intermediate between microscopic and macroscopic scales, where these scales are typically defined specific to each system, and where the mesoscopic scale typically facilitates information between the microscopic and macroscopic scales. Typically, these mesoscopic scales have their own interesting dynamics.

This has been discussed in the SMNI papers with respect to columnar anatomy and physiology in neocortex, which can be described by a nonlinear nonequilibrium multivariate statistical mechanics, a subfield of statistical mechanics dealing with Gaussian Markovian systems with time-dependent drifts and correlated diffusions, with both drifts and diffusions nonlinear in their multiple variables. SMNI has described columnar activity to be an effective mesoscopic scale intermediate between macroscopic regional interactions and microscopic averaged synaptic and neuronal interactions. Such treatment of neuronal activity, beyond pools of individual neurons, is based on evidence over the past 30 years of mesoscopic neocortical columnar anatomy as well as physiology which possess their own dynamics (Mountcastle, 1978; Buxhoeveden & Casanova, 2002). It is important to note that although columnar structure is ubiquitous in neocortex, it is by no means uniform nor is it so simple to define across many areas of the brain (Rakic, 2008). While SMNI has calculated phenomena like STM and EEG to validate this model, there is as yet no specific real columnar data to validate SMNI's precise functional form at this scale.

In this context, while EEG may have generators at microscopic neuronal scales and regional macroscopic scales, this study was motivated to investigate whether mesoscopic scales can support columnar firing activity at observed multiple frequencies, not necessarily generate such frequencies. The short answer is yes. The detailed support of this result requires quite lengthy calculations of the highly nonlinear multivariate SMNI system.

When dealing with stochastic systems, there are several useful tools available when these systems can be described by Gaussian-Markovian probability distributions, even when they are in non-equilibrium, multivariate, and quite nonlinear in their means and variances. SMNI has demonstrated how most likely states described by such distributions can be calculated from the variational principle associated with systems, i.e., as Euler-Lagrange (EL) equations directly from the SMNI Lagrangian (Langouche, Roekaerts & Tirapegui, 1982). This Lagrangian is the argument in the exponent of the SMNI probability distribution. The EL equations are developed from a variational principle applied to this distribution, and

they give rise to a nonlinear string model used by many neuroscientists to describe global oscillatory activity (Ingber, 1995a).

Section 2 is a brief review of the SMNI model relevant to the calculations presented here. It is obvious that the mammalian brain is complex and processes information at many scales, and it has many interactions with sub-cortical structures. SMNI is appropriate to just a few scales and deals primarily with cortical structures. While SMNI has included some specific regional circuitry to address EEG calculations discussed below, details of laminar structure within minicolumns have not been included. Such laminar circuitry is of course important to many processes and, as stated in previous SMNI papers, it can be included by adding more variables. Some laminar structure is implicitly assumed in phenomena discussed in the last two sections dealing with electromagnetic phenomena that depends on some systematic alignment of pyramidal neurons. Care has been taken to test SMNI at the appropriate scales, by calculating experimentally observed phenomena, and to some readers it may be surprising that it is so reasonably successful in these limited endeavors. The mathematics used is from a specialized area of multivariate nonlinear nonequilibrium statistical mechanics (Langouche, Roekaerts & Tirapegui, 1982), and SMNI was the first physical application of these methods to the brain. In this paper, the mathematics used in all SMNI publications is not repeated, albeit referenced, but only enough mathematics is used to deal with the topic being presented.

Section 3 presents calculations of the EL equations, which are based on direct calculations of the nonlinear multivariate EL equations of the SMNI Lagrangian, giving most likely states of the system, performed for three prototypical Cases, dominate excitatory columnar firings, dominate inhibitory columnar firings, and in between balanced columnar firings, with and without a Centering Mechanism (CM) turned on which pulls more stable states into the physical firings ranges. This CM expresses experimentally observed changes in stochastic background of presynaptic interactions during selective attention. These calculations are repeated for the visual neocortex, which has twice as many neurons/minicolumn as other neocortical regions.

Section 4 takes an opportunity here to identify and correct a $\sqrt{2}$ error in the original SMNI work which has been propagated in over 30 papers up until now. This error does not affect any conclusions of previous results, but it must be corrected. Direct comparisons are made using EL results, which also presents an opportunity to see how robust the SMNI model is with respect to changes in synaptic parameters within their experimentally observed ranges.

Section 5 presents calculations of oscillatory states. Using the EL calculations, investigations are performed for each of the prototypical Cases to see if and where oscillatory behavior is observed within experimentally observed ranges.

Section 6 notes that the CM is effective at levels of 10^{-2} or 10^{-3} of the Lagrangian defining a small scale for columnar interactions, i.e., zooming in to still within classical (not quantum) domains of information. If indeed there are quantum scales of direct interaction with classical scales of neuronal activity, it is suggested that the presynaptic background responsible for the CM is a possible area for future investigations.

Section 7 is the Conclusion, offering some conjecture on the utility of having columnar activity support oscillatory frequencies observed over regions of neocortex, e.g., to support conveying local neuronal information across regions as is observed in normal human activity. Mention is made on the importance of including STM in discussions of neural correlates of consciousness.

2. SMNI

Neocortex has evolved to use minicolumns of neurons interacting via short-ranged interactions in macrocolumns, and interacting via long-ranged interactions across regions of macrocolumns. This common architecture processes patterns of information within and among different regions, e.g., sensory, motor, associative cortex, etc.

2.1. SMNI on STM and EEG

A statistical mechanics of neocortical interactions (SMNI) for human neocortex has been developed, building from synaptic interactions to minicolumnar, macrocolumnar, and regional interactions in

neocortex (Ingber, 1982; Ingber, 1983). Over a span of about 30 years, a series of about 30 papers on the statistical mechanics of neocortical interactions (SMNI) has been developed to model columns and regions of neocortex, spanning mm to cm of tissue.

As depicted in Figure 1, SMNI develops three biophysical scales of neocortical interactions: (a)-(a^{*})-(a') microscopic neurons (Sommerhoff, 1974); (b)-(b') mesocolumnar domains (Mountcastle, 1978); (c)-(c') macroscopic regions. SMNI has developed conditional probability distributions at each level, aggregating up several levels of interactions. In (a^{*}) synaptic inter-neuronal interactions, averaged over by mesocolumns, are phenomenologically described by the mean and variance of a distribution Ψ (both Poisson and Gaussian distributions were considered, giving similar results). Similarly, in (a) intraneuronal transmissions are phenomenologically described by the mean and variance of Γ (a Gaussian distribution). Mesocolumnar averaged excitatory (E) and inhibitory (I) neuronal firings M are represented in (a'). In (b) the vertical organization of minicolumns is sketched together with their horizontal stratification, yielding a physiological entity, the mesocolumn. In (b') the overlap of interacting mesocolumns at locations r and r' from times t and $t + \tau$ is sketched. Here $\tau \sim 10$ msec represents typical periods of columnar firings. This reflects on typical individual neuronal refractory periods of ~ 1 msec, during which another action potential cannot be initiated, and a relative refractory period of ~ 0.5 — 10 msec. Future research should determine which of these neuronal time scales are most dominant at the columnar time scale taken to be τ . In (c) macroscopic regions of neocortex are depicted as arising from many mesocolumnar domains. (c') sketches how regions may be coupled by long-ranged interactions.

Most of these papers have dealt explicitly with calculating properties of STM and scalp EEG in order to test the basic formulation of this approach (Ingber, 1981; Ingber, 1982; Ingber, 1983; Ingber, 1984; Ingber, 1985a; Ingber, 1985b; Ingber, 1986b; Ingber & Nunez, 1990; Ingber, 1991; Ingber, 1992; Ingber, 1994; Ingber & Nunez, 1995; Ingber, 1995a; Ingber, 1995b; Ingber, 1996b; Ingber, 1996a; Ingber, 1997; Ingber, 1998). The SMNI modeling of local mesocolumnar interactions, i.e., calculated to include convergence and divergence between minicolumnar and macrocolumnar interactions, was tested on STM phenomena. The SMNI modeling of macrocolumnar interactions across regions was tested on EEG phenomena.

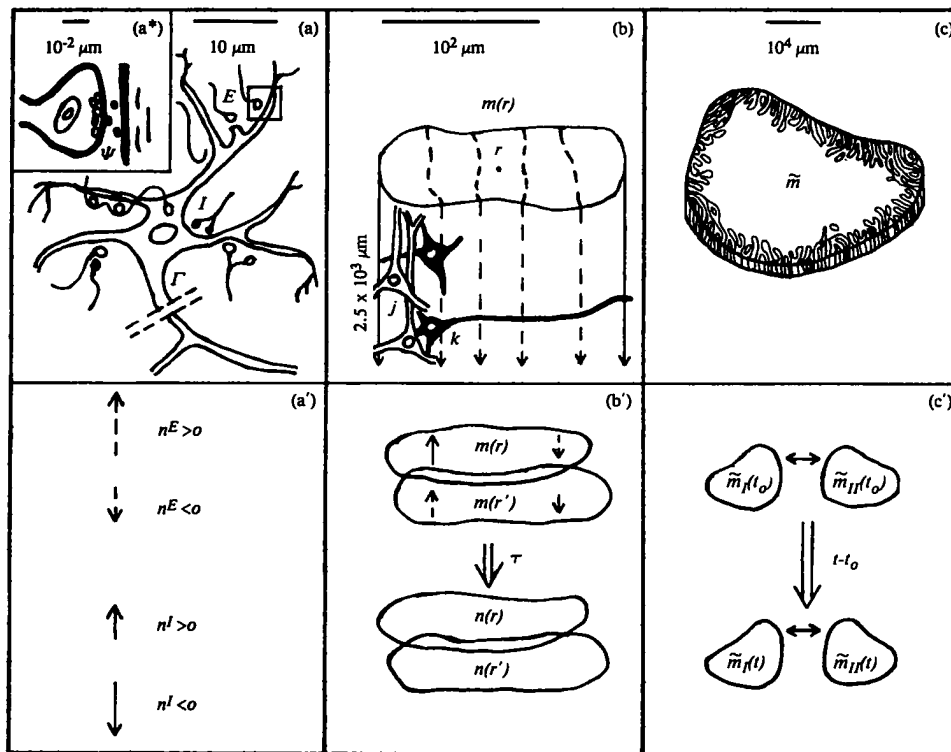


Fig. 1. Illustrated are three biophysical scales of neocortical interactions: (a)-(a^{*})-(a') microscopic neurons; (b)-(b') mesocolumnar domains; (c)-(c') macroscopic regions. by the American Physical Society.

The EEG studies in previous SMNI applications were focused on regional scales of interactions. The STM applications were focused on columnar scales of interactions. However, this EEG study is focused at columnar scales, and it is relevant to stress the successes of this SMNI at this columnar scale, giving additional support to this SMNI model in this context. A previous report considered oscillations in quasi-linearized EL equations (Ingber, 2009a), while this study considers the full nonlinear system.

2.2. SMNI STM

SMNI studies have detailed that maximal numbers of attractors lie within the physical firing space of M^G , where $G = \{\text{Excitatory, Inhibitory}\} = \{E, I\}$ minicolumnar firings, consistent with experimentally observed capacities of auditory and visual STM, when a Centering mechanism (CM) is enforced by shifting background noise in synaptic interactions, consistent with experimental observations under conditions of selective attention (Mountcastle, Andersen & Motter, 1981; Ingber, 1984; Ingber, 1985b; Ingber, 1994; Ingber & Nunez, 1995). This leads to all attractors of the short-time distribution lying approximately along a diagonal line in M^G space, effectively defining a narrow parabolic trough containing these most likely firing states. This essentially collapses the two-dimensional M^G space down to a one-dimensional space of most importance. Thus, the predominant physics of STM and of (short-fiber contribution to) EEG phenomena takes place in this narrow parabolic trough in M^G space, roughly along a diagonal line (Ingber, 1984).

These calculations were further supported by high-resolution evolution of the short-time conditional-probability propagator using a numerical path-integral code, PATHINT (Ingber & Nunez, 1995). SMNI correctly calculated the stability and duration of STM, the observed 7 ± 2 capacity rule of auditory memory and the observed 4 ± 2 capacity rule of visual memory (Ericsson & Chase, 1982; Zhang & Simon, 1985; Ingber, 1984; Ingber, 1985b), the primacy versus recency rule (Ingber, 1995b), random access to memories within tenths of a second as observed, and Hick's law of linearity of reaction time with STM information (Hick, 1952; Jensen, 1987; Ingber, 1999).

SMNI also calculates how STM patterns (e.g., from a given region or even aggregated from multiple regions) may be encoded by dynamic modification of synaptic parameters (within experimentally observed ranges) into long-term memory patterns (LTM) (Ingber, 1983).

2.3. SMNI EEG

Using the power of this formal structure, sets of EEG and evoked potential data from a separate NIH study, collected to investigate genetic predispositions to alcoholism, were fitted to an SMNI model on a lattice of regional electrodes to extract brain signatures of STM (Ingber, 1997; Ingber, 1998). Each electrode site was represented by an SMNI distribution of independent stochastic macrocolumnar-scaled M^G variables, interconnected by long-ranged circuitry with delays appropriate to long-fiber communication in neocortex. The global optimization algorithm Adaptive Simulated Annealing (ASA) (Ingber, 1989; Ingber, 1993a) was used to perform maximum likelihood fits of Lagrangians defined by path integrals of multivariate conditional probabilities. Canonical momenta indicators (CMI), the momentum components of the EL equations, were thereby derived for individual's EEG data. The CMI give better signal recognition than the raw data, and were used to advantage as correlates of behavioral states. In-sample data was used for training (Ingber, 1997), and out-of-sample data was used for testing (Ingber, 1998) these fits.

These results gave strong quantitative support for an accurate intuitive picture, portraying neocortical interactions as having common algebraic physics mechanisms that scale across quite disparate spatial scales and functional or behavioral phenomena, i.e., describing interactions among neurons, columns of neurons, and regional masses of neurons.

2.4. Chaos

There are many papers on the possibility of chaos in neocortical interactions, including some that consider noise-induced interactions (Zhou & Kurths, 2003). While this phenomena may have some merit when dealing with small networks of neurons, e.g., in some circumstances such as epilepsy, these papers generally have considered only too simple models of neocortex. Note that SMNI can be useful to describe some forms of epilepsy, e.g., when columnar firings reach upper limits of maximal firings, as in some of the models presented below (Ingber, 1988).

The author took a model of chaos that might be measured by EEG, developed and published by colleagues (Nunez & Srinivasan, 1993; Srinivasan & Nunez, 1993), but adding background stochastic influences and parameters that were agreed to better model neocortical interactions. The resulting multivariate nonlinear conditional probability distribution was propagated many thousands of epochs, using the authors PATHINT code, to see if chaos could exist and persist under such a model (Ingber, Srinivasan & Nunez, 1996). There was absolutely no measurable instance of chaos surviving in this more realistic context. Note that this study was at the columnar scale, not the finer scales of activity of smaller pools of neurons.

2.5. Mathematics

2.5.1. Background

A spatial-temporal lattice-field short-time conditional multiplicative-noise (nonlinear in drifts and diffusions) multivariate Gaussian-Markovian probability distribution was developed faithful to neocortical function/physiology. Such probability distributions are basic to the SMNI approach used here. The SMNI model was the first physical application of a nonlinear multivariate calculus developed by other mathematical physicists in the late 1970's to define a statistical mechanics of multivariate nonlinear nonequilibrium systems (Graham, 1977; Langouche, Roekaerts & Tirapegui, 1982).

This formulation of a multivariate nonlinear nonequilibrium system requires derivation in a proper Riemannian geometry to study proper limits of short-time conditional probability distributions. Prior to the late 1970's and early 1980's, many uses of path integrals for multivariate systems nonlinear in their drifts and diffusions were too cavalier in taking continuum limits. In general, results of derivations may be formally written as continuum limits, but these should be understood to be implemented as discrete in

derivations as well as in numerical work (Langouche, Roekaerts & Tirapegui, 1982; Schulman, 1981).

Some spin-offs from this study included applications to specific disciplines such as neuroscience (SMNI), finance (Ingber, 1990; Ingber, 2000), combat simulations (Ingber, 1993b), and nuclear physics (Ingber, 1986a). In addition generic computational tools were developed to handle such nonlinear structures, for optimization and importance-sampling with ASA (Ingber, 1993a), and for path-integral systems, including PATHINT (Ingber, 2000; Ingber & Nunez, 1995) and PATHTREE (Ingber, Chen, Mondescu *et al*, 2001). The use of financial risk-management algorithms has been cast into a framework that can enhance resolution of brain imaging from multiple synchronized sources (Ingber, 2008b; Ingber, 2009b). The SMNI model also has been generalized to a model for Artificial Intelligence (Ingber, 2007; Ingber, 2008a).

2.5.2. SMNI Application

Some of the algebra behind SMNI depicts variables and distributions that populate each representative macrocolumn in each region. While Riemannian terms were calculated when using the Stratonovich midpoint discretization of the probability distribution (Ingber, 1982; Ingber, 1983), in order to explicitly deal with the multivariate nonlinearities, here it suffices to use the more readable Ito prepoint discretization, which is an equivalent numerical distribution when used consistently (Langouche, Roekaerts & Tirapegui, 1982).

A derived mesoscopic Lagrangian L defines the short-time probability distribution P of firings in a minicolumn composed of $\sim 10^2$ neurons, where P is the product of P^G , where $G = \{E, I\}$ chemically independent excitatory and inhibitory firing distributions, by aggregating probability distributions of neuronal firings p_{σ_j} , given its just previous interactions with all other neurons in its macrocolumnar surround. \bar{G} designates contributions from both E and I . The Einstein summation convention is used for G indices, whereby repeated indices in a term implies summation over that index, unless summation is prevented by vertical bars, e.g., $|G|$.

$$\begin{aligned}
P &= \prod_G P^G [M^G(r; t + \tau) | M^{\bar{G}}(r'; t)] \\
&= \sum_{\sigma_j} \delta \left(\sum_{jE} \sigma_j - M^E(r; t + \tau) \right) \delta \left(\sum_{jI} \sigma_j - M^I(r; t + \tau) \right) \prod_j^N p_{\sigma_j} \\
&\approx \prod_G (2\pi\tau g^{GG})^{-1/2} \exp(-N\tau L^G), \\
P &\approx (2\pi\tau)^{-1/2} g^{1/2} \exp(-N\tau L), \\
L &= L^E + L^I = (2N)^{-1} (\dot{M}^G - g^G) g_{GG'} (\dot{M}^{G'} - g^{G'}) + M^G J_G / (2N\tau) - V', \\
\dot{M}^G &= [M^G(t + \tau) - M^G(t)] / \tau, \\
V' &= \sum_G V''_{G'} (\rho \nabla M^{G'})^2, \\
g^G &= -\tau^{-1} (M^G + N^G \tanh F^G), \\
g^{GG'} &= (g_{GG'})^{-1} = \delta_G^{G'} \tau^{-1} N^G \text{sech}^2 F^G, \\
g &= \det(g_{GG'}), \\
F^G &= \frac{(V^G - a_{G'}^{|G|} v_{G'}^{|G|} N^{G'} - \frac{1}{2} A_{G'}^{|G|} v_{G'}^{|G|} M^{G'})}{((\pi/2)[(v_{G'}^{|G|})^2 + (\phi_{G'}^{|G|})^2](a_{G'}^{|G|} N^{G'} + \frac{1}{2} A_{G'}^{|G|} M^{G'}))^{1/2}},
\end{aligned}$$

$$a_{G'}^G = \frac{1}{2} A_{G'}^G + B_{G'}^G \quad (1)$$

where $A_{G'}^G$ and $B_{G'}^G$ are minicolumnar-averaged inter-neuronal synaptic efficacies (4 combinations of $\{E, I\}$ with $\{E', I'\}$ firings), $v_{G'}^G$ and $\phi_{G'}^G$ are averaged means and variances of contributions to neuronal electric polarizations. $M^{G'}$ and $N^{G'}$ in F^G are afferent macrocolumnar firings, scaled to efferent minicolumnar firings by $N/N^* \sim 10^{-3}$, where N^* is the number of neurons in a macrocolumn, $\sim 10^5$. Similarly, $A_{G'}^G$ and $B_{G'}^G$ have been scaled by $N^*/N \sim 10^3$ to keep F^G invariant. V' are derived mesocolumnar nearest-neighbor (NN) interactions (not used in this columnar study). J_G was used in early papers to model influences on minicolumnar firings from long-ranged fibers across regions, but later papers integrated these long-ranged fibers directly into the above framework as described below, leaving SMNI with no free parameters. Reasonable typical values of the postsynaptic neuronal parameters are taken to be $|v_{G'}^G| = \phi_{G'}^G = 0.1N^*/N$. The presynaptic neuronal parameters are given below for the different Cases considered.

It is interesting to note that, as originally derived (Ingber, 1982; Ingber, 1983), the numerator of F^G contains information derived from presynaptic firing interactions. The location of most stable states of this SMNI system are highly dependent on the interactions presented in this numerator. The denominator of F^G contains information derived from postsynaptic neuromodular and electrical processing of these firings. The nonlinearities present in this denominator dramatically affect the number and nature of stable states at scales zoomed in at magnifications on the order of a thousand times, representing neocortical processing of detailed information within a sea of stochastic activity.

To properly deal with multivariate nonlinear multiplicative-noise systems, researchers have had to properly discretize the Feynman Lagrangian, L_F , in terms of the Feynman Action \tilde{S}_F , including Riemannian induced with the Stratonovich midpoint discretization (Langouche, Roekaerts & Tirapegui, 1982). Again, the Einstein convention of summing over factors with repeated indices is assumed. The Feynman probability distribution over the entire cortex, consisting of Λ mesocolumns spanning a total cortical area Ω , can be written formally, i.e., with discretization understood to be necessary in all derived uses and numerical calculations, as

$$\begin{aligned} \tilde{S}_F &= \min \Lambda \Omega^{-1} \int dt' \int d^2r L_F, \\ L_F &= \frac{1}{2} N^{-1} (\dot{M}^G - h^G) g_{GG'} (M^{G'} - h^{G'}) - V, \\ h^G &= g^G - \frac{1}{2} g^{-1/2} (g^{1/2} g^{GG'})_{,G'}, \\ V &= V' - \left(\frac{1}{2} h_{;G}^G + R/6 \right) / N, \\ V' &= V'^E + V'^I - M^G J_G / (2N\tau), \\ h_{;G}^G &= g^{-1/2} (g^{1/2} h^G)_{,G}, \\ g &= \|g_{GG'}\| = \det(g_{GG'}) = g_{EE} g_{II}, \\ g_{GG'} &= (g^{GG'})^{-1}, \\ R &= g^{-1} (g_{EE,II} + g_{II,EE}) - \frac{1}{2} g^{-2} \times \{g_{II} [g_{EE,E} g_{II,E} + (g_{EE,I})^2] + g_{EE} [g_{II,I} g_{EE,I} + (g_{II,E})^2]\}, \\ [\dots]_{,G} &\equiv (\partial/\partial M^G) [\dots]. \end{aligned} \quad (2)$$

The Riemannian curvature R arises from the nonlinear inverse variance $g_{GG'}$, which is a *bona fide* metric of this parameter space (Graham, 1978). The discretization of the determinant prefactor of the

conditional probability distribution requires additional care (Langouche, Roekaerts & Tirapegui, 1982). The discretization in the prepoint representation is outlined below. All these these terms were calculated and found to be large enough in SMNI to be included in any numerical calculations if this midpoint discretization were to be used (Ingber, 1983).

In this context, note that all derivations of proper distributions as well as all numerical applications in SMNI should be considered to be in discretized representations. Many physics papers portray formal continuum limits, but discretization must be understood, especially in these nonlinear systems. SMNI presents a moderate noise system, e.g., as was used in the Chaos section above. Since numerical solutions of the path integrals, e.g., using PATHINT and PATHTREE, are proportional to factors of the metric (inverse covariance) and τ , discretization is well enforced. The use of ASA for importance and optimization also uses OPTIONS in the code to enforce discrete states, e.g., integers, to well model SMNI columnar firings.

2.5.3. Prototypical Cases

Three Cases of neuronal firings were considered in the first introduction of STM applications of SMNI (Ingber, 1984). Below is a short summary of these details. Note that while it suffices to define these Cases using F^G , the full Lagrangian and probability distribution, upon which the derivation of the EL equations are based, are themselves quite nonlinear functions of F^G , e.g., via hyperbolic trigonometric functions, etc.

Since STM duration is long relative to τ , stationary solutions of the Lagrangian L, \bar{L} , can be investigated to determine how many stable minima $\ll \bar{M}^G \gg$ may simultaneously exist within this duration. Detailed calculations of time-dependent folding of the full time-dependent probability distribution supports persistence of these stable states within SMNI calculations of observed decay rates of STM (Ingber & Nunez, 1995).

It is discovered that more minima of \bar{L} are created, i.e., brought into the physical firing ranges, if the numerator of F^G contains terms only in \bar{M}^G , tending to center \bar{L} about $\bar{M}^G = 0$. That is, B^G is modified such that the numerator of F^G is transformed to

$$F'^G = \frac{-\frac{1}{2} A_{G'}^{|G|} v_{G'}^{|G|} M^{G'}}{((\pi/2)[(v_{G'}^{|G|})^2 + (\phi_{G'}^{|G|})^2](a'_{G'} N^{G'} + \frac{1}{2} A_{G'}^{|G|} M^{G'}))^{1/2}},$$

$$a'_{G'} = \frac{1}{2} A_{G'}^G + B_{G'}^G, \quad (3)$$

The most likely states of the centered systems lie along diagonals in M^G space, a line determined by the numerator of the threshold factor in F^E , essentially

$$A_E^E M^E - A_I^E M^I \approx 0, \quad (4)$$

noting that in F^I $I-I$ connectivity is experimentally observed to be very small relative to other pairings, so that $(A_E^I M^E - A_I^I M^I)$ is typically small only for small M^E .

Of course, any mechanism producing more as well as deeper minima is statistically favored. However, this particular CM has plausible support: $M^G(t + \tau) = 0$ is the state of afferent firing with highest statistical weight. I.e., there are more combinations of neuronal firings, $\sigma_j = \pm 1$, yielding this state than any other $M^G(t + \tau)$, e.g., $\sim 2^{N^G+1/2} (\pi N^G)^{-1/2}$ relative to the states $M^G = \pm N^G$. Similarly, $M^G(t)$ is the state of efferent firing with highest statistical weight. Therefore, it is natural to explore mechanisms which favor common highly weighted efferent and afferent firings in ranges consistent with favorable firing threshold factors $F^G \approx 0$.

A model of dominant inhibition describes how minicolumnar firings are suppressed by their neighboring minicolumns. For example, this could be effected by developing NN mesocolumnar interactions (Ingber, 1983), but here the averaged effect is established by inhibitory mesocolumns (Case I) by setting $A_E^I = A_I^E = 2A_E^E = 0.01N^*/N$. Since there appears to be relatively little $I-I$ connectivity, set $A_I^I = 0.0001N^*/N$. The background synaptic noise is taken to be $B_I^E = B_E^I = 2B_E^E = 10B_I^I = 0.002N^*/N$.

As minicolumns are observed to have ~ 110 neurons (visual cortex appears to have approximately twice this density) (Mountcastle, 1978), and as there appear to be a predominance of E over I neurons (Nunez, 1981), here take $N^E = 80$ and $N^I = 30$. Use $N^*/N = 10^3$, v_G^G , and ϕ_G^G as estimated previously. \bar{M}^G represents time-averaged M^G . The threshold factors F_I^G for this I model are then

$$F_I^E = \frac{(0.5\bar{M}^I - 0.25\bar{M}^E + 3.0)}{(\pi/2)^{1/2}(0.1\bar{M}^I + 0.05\bar{M}^E + 9.80)^{1/2}},$$

$$F_I^I = \frac{(0.005\bar{M}^I - 0.5\bar{M}^E - 45.8)}{(\pi/2)^{1/2}(0.001\bar{M}^I + 0.1\bar{M}^E + 11.2)^{1/2}}. \quad (5)$$

In the prepoint-discretized deterministic limit, the threshold factors determine when and how smoothly the step-function forms $\tanh F_I^G$ in $g^G(t)$ change $M^G(t)$ to $M^G(t + \tau)$. F_I^I will cause afferent \bar{M}^I to fire for most of its values, as $\bar{M}^I \sim -N^I \tanh F_I^I$ will be positive for most values of \bar{M}^G in F_I^I , which is already weighted heavily with a term -45.8 . Looking at F_I^E , it is seen that the relatively high positive values of efferent \bar{M}^I require at least moderate values of positive efferent \bar{M}^E to cause firings of afferent \bar{M}^E . The use of $\pi/2$ will be discussed below, as this differs from the use of π in previous papers.

The centering effect of the I model, labeled here as the IC model, is quite easy for neocortex to accommodate. For example, this can be accomplished simply by readjusting the synaptic background noise from B_E^G to $B_E'^G$,

$$B_E'^G = \frac{[V^G - (\frac{1}{2} A_I^G + B_I^G)v_I^G N^I - \frac{1}{2} A_E^G v_E^G N^E]}{v_E^G N^G} \quad (6)$$

for both $G = E$ and $G = I$. In general, B_E^G and B_I^G (and possibly A_E^G and A_I^G due to actions of neuromodulators, and J_G constraints from long-ranged fibers) are available to zero the constant in the numerator, giving an extra degree(s) of freedom to this mechanism. (If $B_E'^G$ would be negative, this leads to unphysical results in the square-root denominator of F^G . In all examples where this occurs, it is possible to instead find positive $B_I'^G$ to appropriately shift the numerator of F^G .) In this context, it is empirically observed that the synaptic sensitivity of neurons engaged in selective attention is altered, presumably by the influence of chemical neuromodulators on postsynaptic neurons at their presynaptic sites (Mountcastle, Andersen & Motter, 1981).

By this CM, $B_E'^E = 1.38$ and $B_I'^I = 15.3$, and F_I^G is transformed to F_{IC}^G , Case IC,

$$F_{IC}^E = \frac{(0.5\bar{M}^I - 0.25\bar{M}^E)}{(\pi/2)^{1/2}(0.1\bar{M}^I + 0.05\bar{M}^E + 10.4)^{1/2}},$$

$$F_{IC}^I = \frac{(0.005\bar{M}^I - 0.5\bar{M}^E)}{(\pi/2)^{1/2}(0.001\bar{M}^I + 0.1\bar{M}^E + 20.4)^{1/2}}. \quad (7)$$

Note that, aside from the enforced vanishing of the constant terms in the numerators of F_I^G , the only other changes in F_I^G moderately affect the constant terms in the denominators.

The other extreme of normal neocortical firings is a model of dominant excitation, effected by establishing excitatory mesocolumns (Case E) by using the same parameters $\{B_G^G, v_G^G, \phi_G^G, A_I^I\}$ as in the I model, but setting $A_E^E = 2A_E^I = 2A_I^I = 0.01N^*/N$. This yields

$$F_E^E = \frac{(0.25\bar{M}^I - 0.5\bar{M}^E - 24.5)}{(\pi/2)^{1/2}(0.05\bar{M}^I + 0.10\bar{M}^E + 12.3)^{1/2}},$$

$$F_E^I = \frac{(0.005\bar{M}^I - 0.25\bar{M}^E - 25.8)}{(\pi/2)^{1/2}(0.001\bar{M}^I + 0.05\bar{M}^E + 7.24)^{1/2}}. \quad (8)$$

The negative constant in the numerator of F_E^I inhibits afferent \bar{M}^I firings. Although there is also a

negative constant in the numerator of F_E^E , the increased coefficient of \bar{M}^E (relative to its corresponding value in F_I^E), and the fact that \bar{M}^E can range up to $N^E = 80$, readily permits excitatory firings throughout most of the range of \bar{M}^E .

Applying the CM to E, $B_I^E = 10.2$ and $B_I^I = 8.62$. The net effect in F_{EC}^G , Case EC, in addition to removing the constant terms in the numerators of F_E^G , is to change the constant terms in the denominators: 12.3 in F_E^E is changed to 17.2 in F_{EC}^E , and 7.24 in F_E^I is changed to 12.4 in F_{EC}^I .

Now it is natural to examine a balanced Case intermediate between I and E, labeled here as Case B. This is accomplished by changing $A_E^E = A_E^I = A_I^E = 0.005N^*/N$. This yields

$$F_B^E = \frac{(0.25\bar{M}^I - 0.25\bar{M}^E - 4.50)}{(\pi/2)^{1/2}(0.050\bar{M}^E + 0.050\bar{M}^I + 8.30)^{1/2}},$$

$$F_B^I = \frac{(0.005\bar{M}^I - 0.25\bar{M}^E - 25.8)}{(\pi/2)^{1/2}(0.001\bar{M}^I + 0.050\bar{M}^E + 7.24)^{1/2}}. \quad (9)$$

Applying the CM to B, $B_E^E = 0.438$ and $B_I^I = 8.62$. The net effect in F_{BC}^G , Case BC, in addition to removing the constant terms in the numerators of F_B^G , is to change the constant terms in the denominators: 8.30 in F_B^E is changed to 7.40 in F_{BC}^E , and 7.24 in F_B^I is changed to 12.4 in F_{BC}^I .

Previously, calculations were performed for the three prototypical firing Cases, dominate excitatory (E), dominate inhibitory (I) and balanced about evenly (B). More minima were brought within physical firing ranges when a CM is invoked (Ingber, 1984), by tuning the presynaptic stochastic background, a phenomena observed during selective attention, giving rise to Cases EC, IC and BC. The states BC are observed to yield properties of auditory STM, e.g., the 7 ± 2 capacity rule and times of duration of these memory states (Ingber, 1984; Ingber, 1985b).

It is observed that visual neocortex has twice the number of neurons per minicolumn as other regions of neocortex. In the SMNI model this gives rise to fewer and deeper STM states, consistent with the observed 4 ± 2 capacity rule of these memory states. These calculations are Cases ECV, ICV and BCV.

2.5.4. Macroscopic Circuitry

The most important features of this development are described by the Lagrangian L in the negative of the argument of the exponential describing the probability distribution, and the threshold factor F^G describing an important sensitivity of the distribution to changes in its variables and parameters.

To more properly include long-ranged fibers, when it is possible to include interactions among macrocolumns, the J_G terms can be dropped, and more realistically replaced by a modified threshold factor F^G ,

$$F^G = \frac{(V^G - a_{G'}^{[G]} v_{G'}^{[G]} N^{G'} - \frac{1}{2} A_{G'}^{[G]} v_{G'}^{[G]} M^{G'} - a_{E'}^{\dagger E} v_{E'}^E N^{\dagger E'} - \frac{1}{2} A_{E'}^{\dagger E} v_{E'}^E M^{\dagger E'})}{((\pi/2)[(v_{G'}^{[G]})^2 + (\phi_{G'}^{[G]})^2](a_{G'}^{[G]} N^{G'} + \frac{1}{2} A_{G'}^{[G]} M^{G'} + a_{E'}^{\dagger E} N^{\dagger E'} + \frac{1}{2} A_{E'}^{\dagger E} M^{\dagger E'})^{1/2}}$$

$$a_{E'}^{\dagger E} = \frac{1}{2} A_{E'}^{\dagger E} + B_{E'}^{\dagger E}. \quad (10)$$

Here, afferent contributions from $N^{\dagger E}$ long-ranged excitatory fibers, e.g., cortico-cortical neurons, have been added, where $N^{\dagger E}$ might be on the order of 10% of N^* : Of the approximately 10^{10} to 10^{11} neocortical neurons, estimates of the number of pyramidal cells range from 1/10 to 2/3. Nearly every pyramidal cell has an axon branch that makes a cortico-cortical connection; i.e., the number of cortico-cortical fibers is of the order 10^{10} .

The long-ranged circuitry was parameterized (with respect to strengths and time delays) in the EEG studies described above (Ingber, 1997; Ingber, 1998). In this way SMNI presents a powerful

computational tool to include both long-ranged global regional activity and short-ranged local columnar activity.

This nature of physiological connectivity among columns even across regions can lead to oscillatory behavior induced among many columns, as will be stressed in the Conclusion after results of this study are described.

3. Euler-Lagrange (EL)

The EL equations are derived from the long-time conditional probability distribution of columnar firings over all cortex, represented by \tilde{M} , in terms of the Action S ,

$$\begin{aligned} \tilde{P}[\tilde{M}(t)]d\tilde{M}(t) &= \int \cdots \int D\tilde{M} \exp(-N\tilde{S}), \\ \tilde{M} &= \{M^{G\nu}\}, \\ \tilde{S} &= \int_{t_0}^t dt' \tilde{L}, \\ \tilde{L} &= \Lambda\Omega^{-1} \int d^2r L, \\ L &= L^E + L^I, \\ D\tilde{M} &= \prod_{s=1}^{u+1} \prod_{\nu=1}^{\Lambda} \prod_G^{E,I} (2\pi dt)^{-1/2} (g_s^\nu)^{1/4} dM_s^{G\nu} \delta[M_t = M(t)] [\delta[M_0 = M(t_0)]], \end{aligned} \quad (11)$$

where ν labels the two-dimensional laminar \vec{r} -space of $\Lambda \sim 5 \times 10^5$ mesocolumns spanning a typical region of neocortex, Ω , (total cortical area $\sim 4 \times 10^{11} \mu\text{m}^2$); and s labels the $u + 1$ time intervals, each of duration $dt \leq \tau$, spanning $(t - t_0)$. At a given value of $(r; t)$, $M = \{M^G\}$.

The path integral has a variational principle, $\delta L = 0$ which gives the EL equations for SMNI (Ingber, 1982; Ingber, 1983). The Einstein convention is used to designate summation over repeated indices, and the following notation for derivatives is used:

$$\begin{aligned} (\cdots)_{;z} &= d(\cdots)/dz, \quad z = \{x, y\}, \\ (\cdots)_{,G} &= \partial(\cdots)/\partial M^G, \quad (\cdots)_{,\dot{G}} = \partial(\cdots)/\partial(dM^G/dt), \\ (\cdots)_{,G_{;z}} &= \partial(\cdots)/\partial(dM^G/dz), \\ (\cdots)_{,\nabla G} &= \hat{x}\partial(\cdots)/\partial(dM^G/dx) + \hat{y}\partial(\cdots)/\partial(dM^G/dy). \end{aligned} \quad (12)$$

The EL equations are:

$$\begin{aligned} \delta L &= 0, \\ \delta_G L &= L_{,G} - \nabla \cdot L_{,\nabla G} - L_{,\dot{G};t} = 0, \\ \nabla \cdot L_{,\nabla G} &= L_{,G_{;z};z} = (L_{,G_{;z},G'}) M^{G'}_{;z} + (L_{,G_{;z},G'_{;z}}) M^{G'}_{;zz} \\ L_{,\dot{G};t} &= (L_{,\dot{G},G'}) \dot{M}^{G'} + (L_{,\dot{G},\dot{G}'}) \ddot{M}^{G'}. \end{aligned} \quad (13)$$

This exhibits the extremum condition as a set of differential equations in the variables $\{M^G, \dot{M}^G, \ddot{M}^G, M^G_{;z}, M^G_{;zz}\}$ in $r - t = (x, y, t)$ space, with coefficients nonlinear in M^G . Note that the V' term for NN interactions in the Lagrangian L will introduce spatial derivative terms that appear in these EL equations.

For a given column this is represented as

$$\begin{aligned}\frac{\partial}{\partial t} \frac{\partial L}{\partial(\partial M^E/\partial t)} - \frac{\partial L}{\partial M^E} &= 0 . \\ \frac{\partial}{\partial t} \frac{\partial L}{\partial(\partial M^I/\partial t)} - \frac{\partial L}{\partial M^I} &= 0 .\end{aligned}\tag{14}$$

The Lagrangian components and EL equations are essentially the counterpart to classical dynamics,

$$\begin{aligned}\text{Mass} &= g_{GG'} = \frac{\partial^2 L}{\partial(\partial M^G/\partial t)\partial(\partial M^{G'}/\partial t)} , \\ \text{Momentum} &= \Pi^G = \frac{\partial L}{\partial(\partial M^G/\partial t)} , \\ \text{Force} &= \frac{\partial L}{\partial M^G} , \\ F - ma = 0: \delta L = 0 &= \frac{\partial L}{\partial M^G} - \frac{\partial}{\partial t} \frac{\partial L}{\partial(\partial M^G/\partial t)} .\end{aligned}\tag{15}$$

To investigate dynamics of multivariate stochastic nonlinear systems, such as neocortex presents, it is not sensible to simply apply simple mean-field theories which assume sharply peaked distributions, since the dynamics of nonlinear diffusions in particular are typically washed out. Here, path integral representations of systems, otherwise equivalently represented by Langevin or Fokker-Planck equations, present elegant algorithms by use of variational principles leading to EL equations (Langouche, Roekaerts & Tirapegui, 1982).

The nonlinear string model mentioned in the Introduction was recovered using the EL equation for the electric potential Φ measured by EEG, considering one firing variable along the parabolic trough of attractor states being proportional to Φ (Ingber & Nunez, 1990). Here, the EL equation includes variation across the spatial extent, x , of columns in regions,

$$\frac{\partial}{\partial t} \frac{\partial L}{\partial(\partial\Phi/\partial t)} + \frac{\partial}{\partial x} \frac{\partial L}{\partial(\partial\Phi/\partial x)} - \frac{\partial L}{\partial\Phi} = 0 .\tag{16}$$

The result is

$$\alpha \frac{\partial^2 \Phi}{\partial t^2} + \beta \frac{\partial^2 \Phi}{\partial x^2} + \gamma \Phi - \frac{\partial F}{\partial \Phi} = 0 .\tag{17}$$

The determinant prefactor g defined above also contains nonlinear details affecting the state of the system. Since g is often a small number, distortion of the scale of L is avoided by normalizing g/g_0 , where g_0 is simply g evaluated at $M^E = M^{\ddagger E'} = M^I = 0$.

If there exist regions in neocortical parameter space such that we can identify $\beta/\alpha = -c^2$, $\gamma/\alpha = \omega_0^2$ (e.g., as explicitly calculated using the CM),

$$\frac{1}{\alpha} \frac{\partial F}{\partial \Phi} = -\Phi f(\Phi) ,\tag{18}$$

then we recover the nonlinear string model.

The most-probable firing states derived variationally from the path-integral Lagrangian as the EL equations represent a reasonable average over the noise in the SMNI system. For many studies, the noise cannot be simply disregarded, as demonstrated in other SMNI STM and EEG studies, but for the purpose here of demonstrating the existence of multiple local oscillatory states that can be identified with EEG frequencies, the EL equations serve very well.

Previous SMNI EEG studies have demonstrated that simple linearized dispersion relations derived from the EL equations support the local generation of frequencies observed experimentally as well as deriving diffusive propagation velocities of information across minicolumns consistent with other experimental studies. The earliest studies simply used a driving force $J_G M^G$ in the Lagrangian to model long-ranged interactions among fibers (Ingber, 1982; Ingber, 1983). Subsequent studies considered regional interactions driving localized columnar activity within these regions (Ingber, 1996b; Ingber, 1997; Ingber, 1998). This study considers self-sustaining EEG activity within columns.

3.1. Maxima, Gnuplot and C

Maxima is a computer code that processes algebraic language (Schelter, 2009). The code also can perform many numerical calculations, although typically with less efficiency than C code. Maxima output can be directly converted to Fortran, and then the f2c utility can be used to generate C code. However, that C code is barely readable and thus hard to maintain. Instead, Maxima output can be directly processed by a few simple Unix scripts to generate very decent standard C code. At all stages, numerical checks were used to be sure the Maxima and C codes were faithful to each other. If the columnar parameters are left unspecified, then some of the EL coefficients can be as long as several hundred thousand lines of code.

A great advantage of using an algebraic language like Maxima over numerical languages like C/C++ is that highly nonlinear expressions can be processed before numerical specifications, often keeping small but important scales intact without losing them to round-off constraints.

The numerical output of Maxima is then developed by Gnuplot (Williams & Kelley, 2008) into graphs presented here.

3.2. Adaptive Simulated Annealing

Adaptive Simulated Annealing (ASA) (Ingber, 1989; Ingber, 1993a) is used to optimize nonlinear parameters, deal with complex constraints, and to importance-sample large spaces of multiple variables.

ASA is a C-language code developed to statistically find the best global fit of a nonlinear constrained non-convex cost-function over a D -dimensional space. This algorithm permits an annealing schedule for “temperature” T , an annealing parameter linked historically to other physical processes, decreasing exponentially in annealing-time k , $T = T_0 \exp(-ck^{1/D})$. The introduction of re-annealing also permits adaptation to changing sensitivities in the multi-dimensional parameter-space. This annealing schedule is faster than fast Cauchy annealing, where $T = T_0/k$, and much faster than Boltzmann annealing, where $T = T_0/\ln k$. ASA has over 100 OPTIONS to provide robust tuning over many classes of nonlinear stochastic systems.

4. sqrt(2) Error

The probability distribution for neuronal firing, dependent on the probability distributions of synaptic interactions, had been calculated prior to SMNI (Shaw & Vasudevan, 1974). The SMNI calculation explicitly detailed physical stages in this derivation and generalized the results to be robust using various distributions (Ingber, 1982; Ingber, 1983). While the first SMNI calculations gave the same final results, via direct communication with the author of the previous work, some error found its way into the first SMNI papers.

At the stage of a straightforward saddle-point calculation (Mathews & Walker, 1970), a $\sqrt{2}$ error has been propagated in a series of papers spanning 1981-2008. As first published in 1982 (Ingber, 1982), in the calculation of the conditional probability of individual neuronal firing, p_{σ_j} ,

$$p_{\sigma_j} = \pi^{-\frac{1}{2}} \int_{(\sigma_j F_j \sqrt{\pi}/2)}^{\infty} dz \exp(-z^2) = \frac{1}{2} [1 - \text{erf}(\sigma_j F_j \sqrt{\pi}/2)],$$

$$F_j = (V_j - \sum_k a_{jk} v_{jk}) / [\pi \sum_{k'} a_{jk'} (v_{jk'}^2 + \phi_{jk'}^2)]^{\frac{1}{2}}. \quad (19)$$

The last equation, F_j should be corrected with a $\sqrt{2}$, as in

$$F_j = (V_j - \sum_k a_{jk} v_{jk}) / [(\pi/2) \sum_{k'} a_{jk'} (v_{jk'}^2 + \phi_{jk'}^2)]^{1/2}. \quad (20)$$

This also similarly affects all mesocolumnar averages over neuronal F_j , yielding F^G factors in subsequent algebra.

In this paper, calculations of the Balanced Centered Case with this $\sqrt{2}$ error is Case BC2, to be compared with calculations of Case BC. This error has no dramatic consequences on other results derived in the above papers. This is because in all these papers, regarding $(v_{jk'}^2 + \phi_{jk'}^2)$, only numerical values of 0.1^2 values have been used for $v_{jk'}^2$ and $\phi_{jk'}^2$. Thus, this would only have the numerical effect of increasing ϕ by a factor of 1.73 (a number not well established experimentally): $0.1^2 + 0.1^2 = 0.02 \rightarrow 2(0.02) = 0.04 = 0.1^2 + \sqrt{0.03^2} = 0.1^2 + 0.173^2$, where $qv_{jk'}$ is the mean and $q\phi_{jk'}^2$ is the variance of Γ , in mV, of the postsynaptic response to q quanta. Therefore, this also presents an opportunity to see how robust the SMNI model is with respect to changes in synaptic parameters within their experimentally observed ranges.

While care has been taken to use only neocortical parameters with values within experimental observations, these values can range substantially, and so any results such as those presented here could be just as reasonable if interpolated or reasonably extrapolated between these two figures.

5. Oscillatory States

To investigate self-sustained oscillatory interactions, in the EL equations the substitution is made

$$M^G \rightarrow M^G \exp(-i\omega_G t) \quad (21)$$

where real ω_G is sought in this study, and where the same notation M^G is used in the ω_G -transformed space. The real part of ω_G represents oscillatory states, while the imaginary part represent attenuation in time of these states. If in fact there are some finite neighborhoods in M^G space that supports real ω , with zero or only modest attenuation, then it can be claimed that these neighborhoods support oscillatory states (Ingber, 2009a). The motivation of this study was to seek such states with zero attenuation within experimentally observed ranges and to see if there could be multiple frequencies spanning observed frequency ranges.

Note that if the time scales of postsynaptic response, τ , is on the order of 10 msec, then $\omega_G \tau$ (which is what is being calculated) on the order of 1 is equivalent to a frequency $\nu_G = \omega_G / (2\pi)$ on the order of 16 cps (Hz), in the observed beta range, close to the range of observed Alpha and Beta rhythms.

5.1. Computation

For further computation, for each Case, each of the two coupled EL equations is further decomposed into real and imaginary parts. Code for each function is developed in Maxima, then converted to C code using Unix scripts, yielding 40 files containing these 40 C functions. Each EL C code is a one long single-equation function of 4 variables, $\{M^G, \omega_G\}$. The code developed by Maxima consists of 4.22M (4.22 million) lines of 248M characters. This code is further processed by Unix scripts to a more efficient C code used in runs of 2.39M lines of 102M characters, or an average of 60K lines for each of the 40 functions. The package of ASA (about 13K lines) and SMNI codes compile and run without errors or warnings with low-level optimization flags -g -Wall on IBM a31p Thinkpads running at 2 GHz, under gcc/g++-4.3.3 under Linux Ubuntu 9.04 with 1 GB RAM, and under gcc-4.3.2 under XP Professional SP3/Cygwin-1.5.25-15 with 2 GB RAM.

For each Case, a cost function is defined as the sum of absolute values of real and imaginary parts of both equations, i.e., a sum of 4 C functions. An M^G mesh is defined by 32 points in M^E and 12 points in M^I . The $M^E: M^I$ ranges are -80:80 and -30:30 in increments of 5 for non-visual Cases, and -160:160 and -60:60 in increments of 10 for visual Cases.

Values of M^E or M^I equal to zero are skipped, as for these points optimization with respect to ω_G are indeterminate, as the zeros multiply the ω_G making optimization meaningless. E.g., the EL equations for

$M^G = 0$ is a constant, independent of ω_G . Since there are obvious strong interactions between M^E and M^I , even if one $M^G \neq 0$ supports oscillations, it would be expected that the other $M^G = 0$ (half the G' neurons in the column are firing) would have some oscillations induced, but the G' oscillations are not calculated here. A decision was made not to optimize with respect to just one ω_G and assume some behavior of the other $\omega_{G'}$ at these points. The meshes closest to these Cases offer reasonable insights into what frequencies are supported in these Cases at these points.

The size of these files pushed the capacity of gcc on these particular computers. Memory became exhausted when optimization flag -O was tried. Even without -O flags, attempts to create functions that combined these functions into the one file with each cost function also exhausted memory, so the cost function calls combinations of 4 of these functions in 4 respective files. Numerical checks made between Maxima and C codes gave at least 6 significant figure agreement in the EL equations.

ASA is used to minimize this cost function with parameters ω_G to less than 0.5, about 5 orders of magnitude less than typical larger absolute values that can be attained without minimization when the ω_G are stable in the search. After some experimentation, good results were obtained by using the ASA algorithm for 500 generated states to get within the regions of global minima, then shunting the code over to the modified Nelder-Mead simplex code that is integrated with the ASA distribution in module FITLOC. The simplex code only improved the ASA results in a few instances. Points that did not converge to 0.5, indicating no good fit was achieved at these mesh points, are not registered on the graphs. It was interesting to see that most of the mesh points that did converge gave values of ω_G around observed frequency ranges. After skipping M^G optimizations as discussed above, this left 3,840 Case calls to ASA and FITLOC, each call representing 500 function evaluations in ASA and from 8 to 500 extra evaluations in FITLOC.

At each point in M^G mesh, the argument $i\omega_G$ induces some symmetries in ω_G space:

$$\text{RealEL}(\omega_E, \omega_I) = \text{RealEL}(-\omega_E, -\omega_I)$$

$$\text{ImagEL}(\omega_E, \omega_I) = -\text{ImagEL}(-\omega_E, -\omega_I) \quad (22)$$

These symmetries were checked to be intact in Maxima even with its floating-point precision in the coefficients of $\{M^G, \omega_G\}$ in the EL equations. Therefore, since the cost function is composed of absolute values of real and imaginary parts, the ranges for the optimization were constrained to $-4.0 \leq \omega_E \leq 4.0$ and $0 \leq \omega_I \leq 4.0$, i.e., quadrants $[-\omega_E: +\omega_I]$ and $[+\omega_E: +\omega_I]$, since the other two quadrants in ω_I space would have the same minima structures. I.e., $[-\omega_E: +\omega_I] = [+\omega_E: -\omega_I]$ and $[+\omega_E: +\omega_I] = [-\omega_E: -\omega_I]$. The range of 4.0 was selected to correspond to about 4 times the Alpha frequency. The additional symmetric ω_G minima were added into the graphs after the optimization calculations.

The numerical calculations were performed on a dedicated Ubuntu computer in about 30 secs per Case per mesh point, about 16 CPU-hrs for all calculations. Gnuplot was used this data to develop the graphs presented here.

5.2. Results

In the following figures, oscillatory states supported by satisfying the EL variational equations are given for all Cases. It is clear that the Cases with the CM robustly support oscillatory behavior in many regions of firing space, whereas Cases without this mechanism do not. Clearly, the presence of attractors, as they shift due to their oscillatory factors, make it more feasible to sustain these oscillations. The left and middle columns graph the populations of ω_E and ω_I independently. The right columns give scatter plots of correlated pairs $\omega_E - \omega_I$ as they are calculated from each set of $E - I$ EL equations. This combination of graphs details areas of M^G as well as correlated values of ω_G which support oscillatory interactions.

Figure 2 gives results for Cases I and IC. Figure 3 gives results for Cases E and EC. Figure 4 gives results for Cases B and BC. Figure 5 gives results for Case BC2 with modified postsynaptic stochastic background as discussed previously. Figure 6 gives results for visual cortex with the CM, Cases ICV, ECV and BCV.

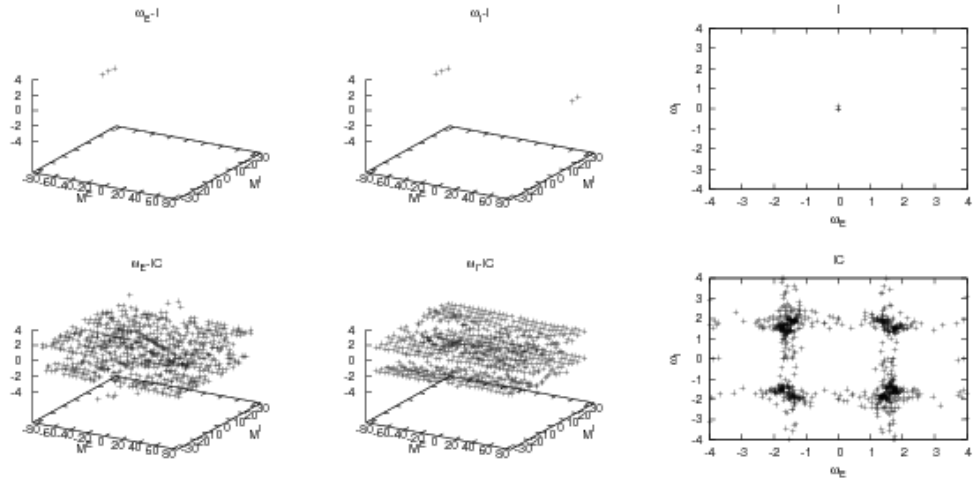


Fig. 2. Oscillatory excitatory firing ω_E and oscillatory inhibitory firing ω_I populations for Case I are in the top left and center graphs, resp. With the CM, ω_E and ω_I for Case IC are in the lower left and center graphs, resp. The right columns give the correlated pairs $\omega_E - \omega_I$ as they are calculated from each set of $E - I$ EL equations.

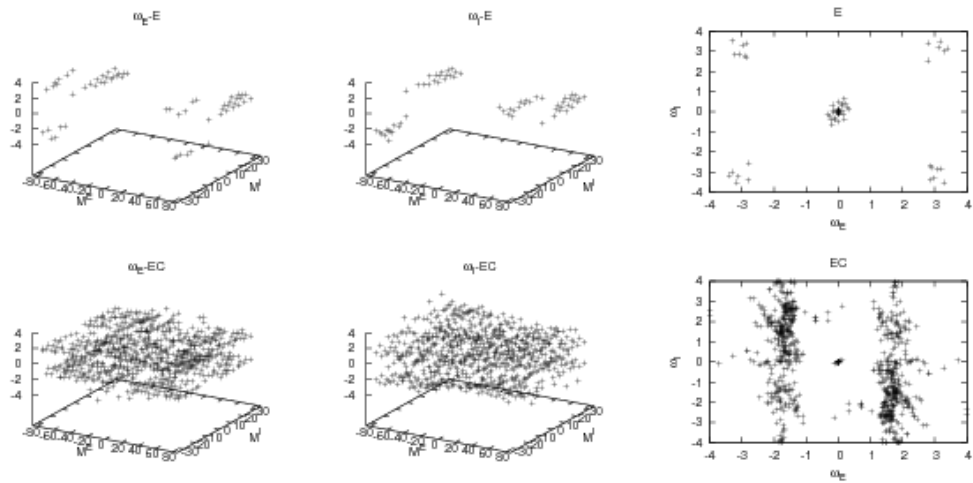


Fig. 3. Oscillatory excitatory firing ω_E and oscillatory inhibitory firing ω_I populations for Case E are in the top left and center graphs, resp. With the CM, ω_E and ω_I for Case EC are in the lower left and center graphs, resp. The right columns give the correlated pairs $\omega_E - \omega_I$ as they are calculated from each set of $E - I$ EL equations.

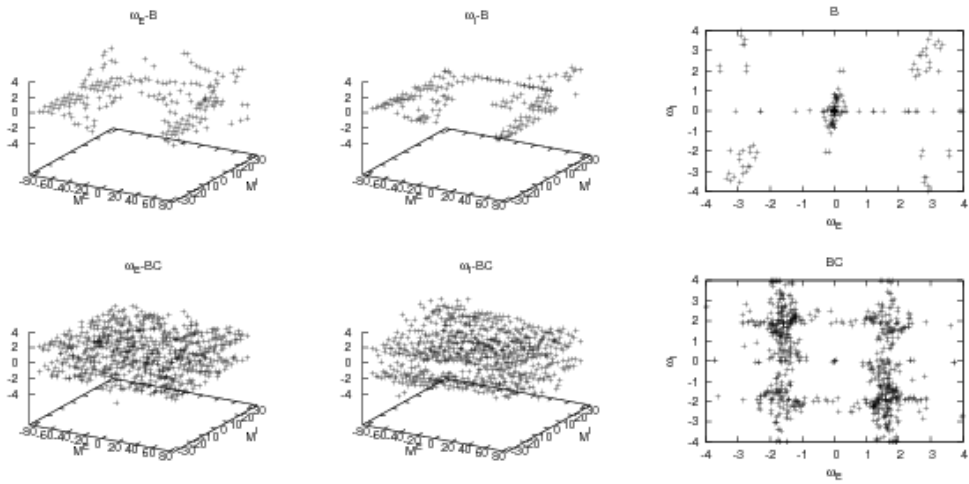


Fig. 4. Oscillatory excitatory firing ω_E and oscillatory inhibitory firing ω_I populations for Case B are in the top left and center graphs, resp. With the CM, ω_E and ω_I for Case BC are in the lower left and center graphs, resp. The right columns give the correlated pairs $\omega_E - \omega_I$ as they are calculated from each set of $E - I$ EL equations.

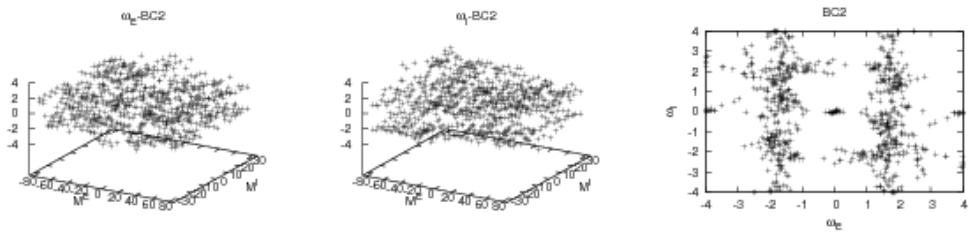


Fig. 5. With the CM, oscillatory excitatory firing ω_E and oscillatory inhibitory firing ω_I populations for Case BC2 are in the left and center graphs, resp. The right columns give the correlated pairs $\omega_E - \omega_I$ as they are calculated from each set of $E - I$ EL equations.

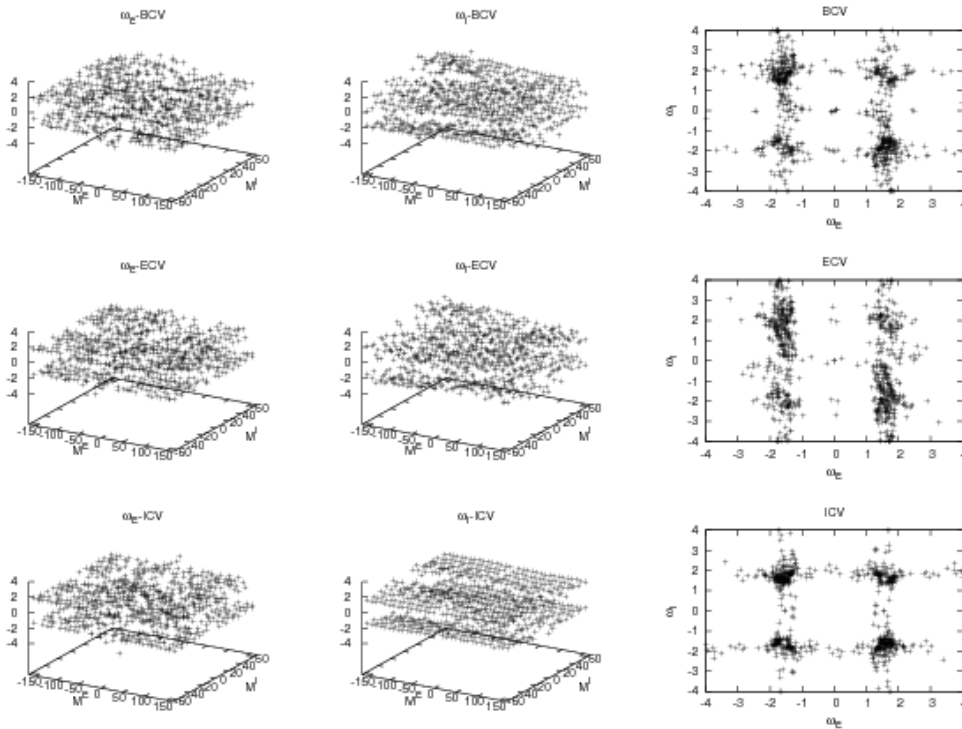


Fig. 6. With the CM, for visual cortex, oscillatory excitatory firings ω_E populations for Cases BCV, ECV and ICV are in the left column, in the top, middle and bottom graphs, resp. Oscillatory inhibitory firings ω_I for Cases BCV, ECV and ICV are in the center column, in the top, middle and bottom graphs, resp. The right columns give the correlated pairs $\omega_E - \omega_I$ as they are calculated from each set of $E - I$ EL equations.

In all CM Cases, there is a high clustering of all observed frequencies, most populated in in the ranges Beta and Gamma, but extending broadly into Alpha as well. In the non-CM Cases, there is not robust support for most observed frequencies, but Delta and Theta are sparsely populated. Note that this interpretation of results is highly sensitive to the details of the time scales of averaged postsynaptic response, τ , which has been chosen here to be on the order of 10 msec,

6. Quantum Influences

The presynaptic CM is effective at levels of 10^{-2} or 10^{-3} of the Lagrangian defining a small scale for columnar interactions, i.e., zooming in to still within classical (not quantum) domains of information. If indeed there are quantum scales of direct interaction with classical scales of neuronal activity, it is suggested that the presynaptic background responsible for the CM is a possible area for future investigations. Previous papers have described how some new columnar interactions might be tested using enhanced resolution from multiple synchronous imaging techniques using SMNI (Ingber, 2008b; Ingber, 2009b). In the context of this paper, a proposed specific quantum influence on classical columnar activity might be tested using such enhanced resolution. This section gives the rationale for the possible nature of such an interaction.

Over the past decades, there is growing evidence that a direct interaction of coherent quantum states with classical scales of interaction, via a mechanism utilizing the superoxide radical $O_2^{\bullet-}$, may be responsible for birds being able to “see” magnetic fields aiding them to navigate over long distances (Kominis, 2009; Rodgers & Hore, 2009; Solov’yov & Schulten, 2009). It should be noted that this is just a proposed mechanism (Johnsen & Lohmann, 2008). However, if indeed such a magnetic mechanism via a superoxide radical has evolved in one higher organism, it may be present in others.

There have been proposed mechanisms that interactions between minicolumns and complex glial networks, involving reciprocal magnetic interaction between neurons and astrocytes, are involved in

cerebral memory and computation (Banachlocha, 2007). This suggests that it is possible that the changes in the presynaptic background responsible for the CM are influenced by magnetic interactions in glial networks. These magnetic interactions would be strongly influenced by changing electrical activity of minicolumnar firings, i.e., columnar EEG as calculated here. In minicolumns there is systematic alignment of pyramidal neurons, which can enhance these magnetic fields. Note that typical values of magnetic fields measured in the human brain, corresponding to auditory evoked potential on the order of $10 \mu\text{V}$ are about 10 pT ($1 \text{ pT} = 1 \text{ pico Tesla} = 10^{-12} \text{ Tesla}$) (Reite & Zimmerman, 1978), but some investigators estimate minicolumnar magnetic fields may reach up to $0.2 \mu\text{T}$ (Banachlocha, 2007). Typical magnetic fields on the Earth's surface are about $30\text{-}60 \mu\text{T}$. Typical magnetic fields used in MRI are $5\text{-}10 \text{ T}$. These ranges illustrate the difficulty in finding a reasonable magnetic mechanism in the brain. However, the brain magnetic mechanism conjectured here would effect background presynaptic noise, not generate any signal per se. The Conclusion further discusses some roles of noise in sometimes helping signal resolution.

For example, a possible scenario might have some columnar activity initiated by external or internal stimuli. Via long-ranged interactions, such changes in this columnar firings would contribute to changes in other columnar firings, even across regions of cortex. If the presynaptic background that turns on the CM was influenced by a glial network via magnetic interactions in turn influenced by oscillatory columnar activity, possibly influenced by increased levels of oxygen due to increased blood flow to more active columns, a sufficiently strong coupled interaction among these mechanisms could be sustained within durations of observed STM, giving rise to observed cerebral memory and computation.

7. Conclusion

Using SMNI, scenarios mentioned above can be detailed. For example, if oscillatory behavior is generated within a given column — especially a column with the CM on, then these oscillations may be induced in other columns — especially those with the CM on and with which it has strong connectivity via long-ranged $M^{\ddagger E'}$ firings which contribute to their local threshold factors F^G . Therefore it is reasonable to conjecture that if columnar firings of short-ranged fibers M^G can oscillate within ranges of oscillations of long-ranged fibers $M^{\ddagger E}$, this could facilitate information processed at fine neuronal and synaptic scales to be carried across minicolumns and regional columns with relative efficiency. Note that this activity is at levels of 10^{-2} or 10^{-3} of the Lagrangian defining a small scale for STM, i.e., zooming in to still within classical (not quantum) domains of information, e.g., at the scale being sensitive to one to several neurons.

While attractor states have been explicitly detailed in previous papers for several SMNI models, here oscillatory states have been calculated throughout the range of firing space. Given that long-ranged fiber interactions across regions can constrain columnar firings, it is useful to at least learn how oscillations may be supported in limited ranges of such constrained firings.

The results show that only under conditions suitable for STM do columnar interactions per se support spectra of oscillatory behavior ω_G in observed frequency ranges robust throughout M^G firing space. In retrospect, this is not too surprising, since some coherent interactions are likely required to sustain multiple stable states for STM. This leads to a strong inference that physiological states of columnar activity receptive to selective attention support oscillatory processing in these ranges. Note that selective attention even to information processed within a given region of neocortex likely requires interactions with frontal cortex and/or sub-cortical structures not explicitly included in the SMNI model.

For example, during Theta — often present during sleep, and during faster Beta and Gamma — often present during intense concentration, information inherent in dynamic STM firings as well as in relatively static LTM synaptic parameters, are often merged into associative neocortex, and during conscious selective attention frontal cortex often controls processing of this information. The use of global carrier frequencies could aid in the noise suppression to convey this information at the finer scales calculated here.

The sensitivity of stochastic multivariate nonlinear (multiple quasi-stable states) to relatively weak oscillatory forces has been documented in many systems (Lindner, Garcia-Ojalvo, Neiman & Schimansky-Geier, 2004). Stochastic resonance has been demonstrated in mammalian brain, using

relatively weak electric fields to effect sinusoidal signals in stochastic firings of groups of neurons (Gluckman, Netoff *et al*, 1996). In SMNI, noise arises at synaptic levels, and the sensitivity at issue in STM is at the aggregated mesoscopic level of columns of neuronal distributions. The averaged synaptic noise is a parameter which appears in the mean as well as the covariance of the aggregated system via the threshold factors F^G . As introduced here at the columnar level, oscillatory changes in firings within the duration of STM shifts the stable STM states in firing space, directly affecting access to these states.

The source of the background synaptic noise, especially presynaptic noise which gives rise to the CM, also is a long-standing area of research (Gluckman, Netoff *et al*, 1996). Further research into the roles of the CM and columnar support for EEG, together with other proposed mechanisms for columnar-glia magnetic interactions for some control of glial-presynaptic background interactions, includes a path for future investigations outlined above to test for quantum-classical interactions that directly support STM by controlling presynaptic noise.

STM (or working memory), along with selective (or focused) attention to this memory, are generally considered important aspects of the “easy” problem of consciousness, e.g., where objective neural correlates of consciousness (NCC) are sought, without addressing the “hard” aspects of subjective and phenomenal states, e.g., “qualia” (Crick & Koch, 1998). In the absence of selective attention, unconscious processing of information and computation can still take place using STM. In this context, such research in consciousness and unconscious information processing must include the dynamics of STM.

It has been demonstrated here at the columnar scale, that both shifts in local columnar presynaptic background as well as local or global regional oscillatory interactions can effect or be affected by attractors that have detailed experimental support to be considered states of STM. This interplay can provide mechanisms for information processing and computation in mammalian neocortex.

Acknowledgments

I thank Andrew Bennett for bringing the $\sqrt{2}$ error to my attention.

References

- Alexander, D.M. (2007) Is the EEG an epiphenomenon?. *J. Neurosci.* 27, 3030-3036. [URL <http://www.jneurosci.org/cgi/eletters/27/11/3030#6000>]
- Alexander, D.M., Arns, M.W., Paul, R.H., Rowe, D.L., Cooper, N., Esser, A.H., Fallahpour, K., Stephan, B.C.M., Hessen, E., Breteler, R., Williams, L.M. & Gordon, E. (2006) EEG markers for cognitive decline in elderly subjects with subjective memory complaints. *J. Integrative Neurosci.* 5(1), 49-74.
- Axmacher, N., Mormann, F., Fernandez, G., Elger, C. & Fell, J. (2006) Memory formation by neuronal synchronization. *Brain Res. Rev.* 52, 170-182.
- Banachlocha, M.A.M. (2007) Neuromagnetic dialogue between neuronal minicolumns and astroglial network: A new approach for memory and cerebral computation. *Brain Res. Bull.* 73, 21-27.
- Buxhoeveden, D.P. & Casanova, M.F. (2002) The minicolumn hypothesis in neuroscience. *Brain.* 125(5), 935-951. [URL <http://tinyurl.com/bc2002brain>]
- Crick, F. & Koch, C. (1998) Consciousness and neuroscience. 8, 97-107. [URL <http://www.klab.caltech.edu/~koch/crick-koch-cc-97.html>]
- Ericsson, K.A. & Chase, W.G. (1982) Exceptional memory. *Am. Sci.* 70, 607-615.
- Gluckman, B.J., Netoff, T.I., Neel, E.J., Ditto, W.L., Spano, M.L. & Schiff, S.J. (1996) Stochastic resonance in a neuronal network from mammalian brain. *Phys. Rev. Lett.* 77(19).
- Graham, R. (1977) Covariant formulation of non-equilibrium statistical thermodynamics. *Z. Physik.* B26, 397-405.
- Graham, R. (1978) Path-integral methods in nonequilibrium thermodynamics and statistics, In: *Stochastic Processes in Nonequilibrium Systems*, ed. L. Garrido, P. Seglar & P.J. Shepherd. Springer, 82-138.
- Hick, W. (1952) On the rate of gains of information. *Quarterly J. Exper. Psychology.* 34(4), 1-33.
- Ingber, L. (1981) Towards a unified brain theory. *J. Social Biol. Struct.* 4, 211-224. [URL http://www.ingber.com/smni81_unified.pdf]
- Ingber, L. (1982) Statistical mechanics of neocortical interactions. I. Basic formulation. *Physica D.* 5, 83-107. [URL http://www.ingber.com/smni82_basic.pdf]
- Ingber, L. (1983) Statistical mechanics of neocortical interactions. Dynamics of synaptic modification. *Phys. Rev. A.* 28, 395-416. [URL http://www.ingber.com/smni83_dynamics.pdf]
- Ingber, L. (1984) Statistical mechanics of neocortical interactions. Derivation of short-term-memory capacity. *Phys. Rev. A.* 29, 3346-3358. [URL http://www.ingber.com/smni84_stm.pdf]
- Ingber, L. (1985a) Statistical mechanics of neocortical interactions. EEG dispersion relations. *IEEE Trans. Biomed. Eng.* 32, 91-94. [URL http://www.ingber.com/smni85_eeg.pdf]
- Ingber, L. (1985b) Statistical mechanics of neocortical interactions: Stability and duration of the 7+-2 rule of short-term-memory capacity. *Phys. Rev. A.* 31, 1183-1186. [URL http://www.ingber.com/smni85_stm.pdf]
- Ingber, L. (1986a) Riemannian contributions to short-ranged velocity-dependent nucleon-nucleon interactions. *Phys. Rev. D.* 33, 3781-3784. [URL http://www.ingber.com/nuclear86_riemann.pdf]
- Ingber, L. (1986b) Statistical mechanics of neocortical interactions. *Bull. Am. Phys. Soc.* 31, 868.
- Ingber, L. (1988) Mesoscales in neocortex and in command, control and communications (C3) systems, In: *Systems with Learning and Memory Abilities: Proceedings, University of Paris 15-19 June 1987*, ed. J. Delacour & J.C.S. Levy. Elsevier, 387-409.
- Ingber, L. (1989) Very fast simulated re-annealing. *Mathl. Comput. Modelling.* 12(8), 967-973. [URL http://www.ingber.com/asa89_vfsr.pdf]
- Ingber, L. (1990) Statistical mechanical aids to calculating term structure models. *Phys. Rev. A.* 42(12), 7057-7064. [URL http://www.ingber.com/markets90_interest.pdf]

- Ingber, L. (1991) Statistical mechanics of neocortical interactions: A scaling paradigm applied to electroencephalography. *Phys. Rev. A.* 44(6), 4017-4060. [URL http://www.ingber.com/smni91_eeg.pdf]
- Ingber, L. (1992) Generic mesoscopic neural networks based on statistical mechanics of neocortical interactions. *Phys. Rev. A.* 45(4), R2183-R2186. [URL http://www.ingber.com/smni92_mnn.pdf]
- Ingber, L. (1993a) Adaptive Simulated Annealing (ASA). Global optimization C-code. Caltech Alumni Association. [URL <http://www.ingber.com/#ASA-CODE>]
- Ingber, L. (1993b) Statistical mechanics of combat and extensions, In: *Toward a Science of Command, Control, and Communications*, ed. C. Jones. American Institute of Aeronautics and Astronautics, 117-149. [ISBN 1-56347-068-3. URL http://www.ingber.com/combata93_c3sci.pdf]
- Ingber, L. (1994) Statistical mechanics of neocortical interactions: Path-integral evolution of short-term memory. *Phys. Rev. E.* 49(5B), 4652-4664. [URL http://www.ingber.com/smni94_stm.pdf]
- Ingber, L. (1995a) Statistical mechanics of multiple scales of neocortical interactions, In: *Neocortical Dynamics and Human EEG Rhythms*, ed. P.L. Nunez. Oxford University Press, 628-681. [ISBN 0-19-505728-7. URL http://www.ingber.com/smni95_scales.pdf]
- Ingber, L. (1995b) Statistical mechanics of neocortical interactions: Constraints on 40 Hz models of short-term memory. *Phys. Rev. E.* 52(4), 4561-4563. [URL http://www.ingber.com/smni95_stm40hz.pdf]
- Ingber, L. (1996a) Nonlinear nonequilibrium nonquantum nonchaotic statistical mechanics of neocortical interactions. *Behavioral and Brain Sci.* 19(2), 300-301. [Invited commentary on Dynamics of the brain at global and microscopic scales: Neural networks and the EEG, by J.J. Wright and D.T.J. Liley. URL http://www.ingber.com/smni96_nonlinear.pdf]
- Ingber, L. (1996b) Statistical mechanics of neocortical interactions: Multiple scales of EEG, In: *Frontier Science in EEG: Continuous Waveform Analysis (Electroencephal. clin. Neurophysiol. Suppl. 45)*, ed. R.M. Dasheiff & D.J. Vincent. Elsevier, 79-112. [Invited talk to Frontier Science in EEG Symposium, New Orleans, 9 Oct 1993. ISBN 0-444-82429-4. URL http://www.ingber.com/smni96_eeg.pdf]
- Ingber, L. (1997) Statistical mechanics of neocortical interactions: Applications of canonical momenta indicators to electroencephalography. *Phys. Rev. E.* 55(4), 4578-4593. [URL http://www.ingber.com/smni97_cmi.pdf]
- Ingber, L. (1998) Statistical mechanics of neocortical interactions: Training and testing canonical momenta indicators of EEG. *Mathl. Computer Modelling.* 27(3), 33-64. [URL http://www.ingber.com/smni98_cmi_test.pdf]
- Ingber, L. (1999) Statistical mechanics of neocortical interactions: Reaction time correlates of the g factor. *Psychology.* 10(068). [Invited commentary on The g Factor: The Science of Mental Ability by Arthur Jensen. URL http://www.ingber.com/smni99_g_factor.pdf]
- Ingber, L. (2000) High-resolution path-integral development of financial options. *Physica A.* 283(3-4), 529-558. [URL http://www.ingber.com/markets00_highres.pdf]
- Ingber, L. (2007) Ideas by Statistical Mechanics (ISM). *J. Integrated Systems Design and Process Science.* 11(3), 31-54. [Special Issue: Biologically Inspired Computing.]
- Ingber, L. (2008a) AI and Ideas by Statistical Mechanics (ISM), In: *Encyclopedia of Artificial Intelligence*, ed. J.R. Rabuñal, J. Dorado & A.P. Pazos. Information Science Reference, 58-64. [ISBN 978-1-59904-849-9]
- Ingber, L. (2008b) Statistical mechanics of neocortical interactions (SMNI): Testing theories with multiple imaging data. *NeuroQuantology Journal.* 6(2), 97-104. [URL [Invited paper http://www.neuroquantology.com/journal/index.php/nq/article/view/186/237](http://www.neuroquantology.com/journal/index.php/nq/article/view/186/237)]
- Ingber, L. (2009a) Statistical mechanics of neocortical interactions: Columnar EEG. Report 2009:CEEG. Lester Ingber Research. [URL http://www.ingber.com/smni09_columnar_eeg.pdf]

- Ingber, L. (2009b) Statistical mechanics of neocortical interactions: Portfolio of physiological indicators. *Open Cybernetics Systemics J.* 3(14), 13-26. [doi: 10.2174/1874110X00903010013]
- Ingber, L., Chen, C., Mondescu, R.P., Muzzall, D. & Renedo, M. (2001) Probability tree algorithm for general diffusion processes. *Phys. Rev. E.* 64(5), 056702-056707. [URL http://www.ingber.com/path01_pathtree.pdf]
- Ingber, L. & Nunez, P.L. (1990) Multiple scales of statistical physics of neocortex: Application to electroencephalography. *Mathl. Comput. Modelling.* 13(7), 83-95.
- Ingber, L. & Nunez, P.L. (1995) Statistical mechanics of neocortical interactions: High resolution path-integral calculation of short-term memory. *Phys. Rev. E.* 51(5), 5074-5083. [URL http://www.ingber.com/smni95_stm.pdf]
- Ingber, L., Srinivasan, R. & Nunez, P.L. (1996) Path-integral evolution of chaos embedded in noise: Duffing neocortical analog. *Mathl. Computer Modelling.* 23(3), 43-53. [URL http://www.ingber.com/path96_duffing.pdf]
- Jensen, A. (1987) Individual differences in the Hick paradigm, In: *Speed of Information-Processing and Intelligence*, ed. P.A. Vernon. Ablex, 101-175.
- Jensen, O. & Lisman, J.E. (2005) Hippocampal sequence-encoding driven by a cortical multi-item working memory buffer. *Trends in Neuroscience.* 28(2), 67-72.
- Johnsen, S. & Lohmann, K.L. (2008) Magnetoreception in animals. *Phys Today.* 61, 29-35.
- Kahana, M.J. (2006) The cognitive correlates of human brain oscillations. *J. Neuro.* 26(6), 1669-1672.
- Kahana, M.J., Seelig, D. & Madsen, J.R. (2001) Theta returns. *Current opinion in neurobiology.* 11, 739-744.
- Kominis, I.K. (2009) Zeno is pro Darwin: quantum Zeno effect suppresses the dependence of radical-ion-pair reaction yields on exchange and dipolar interactions. arXiv:0908.0763v2 [quant-ph]. University of Crete.
- Langouche, F., Roekaerts, D. & Tirapegui, E. (1982) *Functional Integration and Semiclassical Expansions.* Reidel, Dordrecht, The Netherlands.
- Lindner, B., Garcia-Ojalvo, J., Neiman, A. & Schimansky-Geier, L. (2004) Effects of noise in excitable systems. *Phys. Rep.* 392, 321-424.
- Lisman, J.E. & Idiart, M.A.P. (1995) Storage of 7+-2 Short-Term Memories in Oscillatory Subcycles. *Science.* 267(5203), 1512-1515.
- Logar, V., Belìe, A., Koritnik, B., Brezan, S., Zidar, J., Karba, R. & Matko, D. (2008) Using ANNs to predict a subject's response based on EEG traces. *Neural Networks.* 21(7), 881-887.
- Mathews, J. & Walker, R.L. (1970) *Mathematical Methods of Physics*, 2nd ed.. Benjamin, New York, NY.
- Meltzer, J.A., Fonzo, G.A. & Constable, T. (2009) Transverse patterning dissociates human EEG theta power and hippocampal BOLD activation. *Psychophysiology.* 46(1), 153-162.
- Mormann, F., Fell, J., Axmacher, N., Weber, B., Lehnertz, K., Elger, C.E. & Fernandez, G. (2005) Phase / amplitude reset and theta-gamma interaction in the human medial temporal lobe during a continuous word recognition memory task. *Hippocampus.* 15, 890-900.
- Mountcastle, V.B. (1978) An organizing principle for cerebral function: The unit module and the distributed system, In: *The Mindful Brain*, ed. G.M. Edelman & V.B. Mountcastle. Massachusetts Institute of Technology, 7-50.
- Mountcastle, V.B., Andersen, R.A. & Motter, B.C. (1981) The influence of attentive fixation upon the excitability of the light-sensitive neurons of the posterior parietal cortex. *J. Neurosci.* 1, 1218-1235.
- Nunez, P.L. (1974) The brain wave equation: A model for the EEG. *Math. Biosci.* 21, 279-297.
- Nunez, P.L. (1981) *Electric Fields of the Brain: The Neurophysics of EEG.* Oxford University Press, London.

- Nunez, P.L. (1995) *Neocortical Dynamics and Human EEG Rhythms*. Oxford University Press, New York, NY.
- Nunez, P.L. & Srinivasan, R. (1993) Implications of recording strategy for estimates of neocortical dynamics with electroencephalography. *Chaos*. 3(2), 257-266.
- Osipova, D., Takashima, A., Oostenveld, R., Fernandez, G., Maris, E. & Jensen, O. (2006) Theta and gamma oscillations predict encoding and retrieval of declarative memory. *J. Neuro.* 26(28), 7523-7531.
- Radman, T., Su, Y., An, J.H., Parra, L.C. & Bikson, M. (2007) Spike timing amplifies the effect of electric fields on neurons: Implications for endogenous field effects. 27. , 3030-3036.
- Rakic, P. (2008) Confusing cortical columns. *PNAS*. 105(34), 12099-12100. [URL <http://www.pnas.org/content/105/34/12099.full>]
- Reite, M. & Zimmerman, J. (1978) Magnetic phenomena of the central nervous system. *Ann. Rev. Biophys. Engineer.* 7, 167-188.
- Rodgers, C.T. & Hore, P.J. (2009) Chemical magnetoreception in birds: The radical pair mechanism. *PNAS*. 106(2), 353-360.
- Schelter, W. (2009) Maxima. DOE, <http://maxima.sourceforge.net>.
- Schulman, L.S. (1981) *Techniques and Applications of Path Integration*. J. Wiley & Sons, New York.
- Sederberg, P.B., Kahana, M.J., Howard, M.W., Donner, E.J. & Madsen, J.R. (2003) Theta and gamma oscillations during encoding predict subsequent recall. *J. Neuro.* 23(34), 10809-10814.
- Shaw, G.L. & Vasudevan, R. (1974) Persistent states of neural networks and the random nature of synaptic transmission. *Math. Biosci.* 21, 207-218.
- Singer, W. (1999) Neuronal synchrony: a versatile code for the definition of relations?. *Neuron*. 24, 49-65.
- Solov'yov, I.A. & Schulten, K. (2009) Magnetoreception through cryptochrome may involve superoxide. *Biophys. J.* 96(12), 4804-4813.
- Sommerhoff, G. (1974) *Logic of the Living Brain*. Wiley, New York, NY.
- Srinivasan, R. & Nunez, P.L. (1993) Neocortical dynamics, EEG standing waves and chaos, In: *Nonlinear Dynamical Analysis for the EEG*, ed. B.H. Jansen & M. Brandt. World Scientific, 310-355.
- Williams, T. & Kelley, C. (2008) Gnuplot. Dartmouth, <http://gnuplot.sourceforge.net>.
- Zhang, G. & Simon, H.A. (1985) STM capacity for Chinese words and idioms: Chunking and acoustical loop hypotheses. *Memory & Cognition*. 13, 193-201.
- Zhou, C. & Kurths, J. (2003) Noise-induced synchronization and coherence resonance of a Hodgkin-Huxley model of thermally sensitive neurons. *Chaos*. 13, 401-409.